Kinetics of Long Chain Branching in Continuous Solution Polymerization of Ethylene Using Constrained Geometry Metallocene

Wen-Jun Wang, Dajing Yan, Shiping Zhu,* and Archie E. Hamielec

Departments of Chemical Engineering and Materials Science and Engineering, McMaster University, Hamilton, Ontario, Canada L8S 4L7

Received June 9, 1998; Revised Manuscript Received September 8, 1998

ABSTRACT: Our high-temperature and high-pressure continuous stirred-tank reactor (CSTR) has been used for the polymerization of ethylene with the constrained geometry metallocene system, [$C_5Me_4(SiMe_2N^tBu)$]$TiMe_2$ (CGC−Ti)/ tris(pentafluorophenyl)boron (TPFPB)/ modified methylaluminoxane (MMAO), in Isopar E solution at 500 psig. Polyethylenes (PE) with long chain branching (LCB) densities up to 0.44 carbons/10 000 carbons, melt flow index ratios of 7.4−25.7, and narrow polydispersity indexes about 2 were synthesized. The polymerization variables included temperature, mean residence time, and ethylene feed concentration. Polyethylene chains terminated mainly by transfer to monomer yielded macromonomers for the LCB formation. The CGC−Ti catalyst appeared to be single site type, and active centers showed an exponential decay with mean residence time. The rate constants and their activation energies of the ethylene propagation, LCB, chain transfer to monomer, and chain transfer to hydrogen were estimated. The presence of methyl side chains in PEs produced at elevated temperatures indicated that the open structure of CGC−Ti catalyst allowed macromonomers to have 2,1-insertion.

Introduction

Further to the continuous solution polymerization of ethylene utilizing zirconocene dichloride (Cp_2ZrCl_2)/ modified methylaluminoxane (MMAO)/trimethylaluminum (TMA),[1] we report here the polymerization kinetics of ethylene with long chain branching (LCB) using a constrained geometry catalyst (CGC) in our high-pressure and high-temperature continuous stirred-tank reactor (CSTR) system.

Compared to the linear polymers having the same average molecular weight, LCB polymers have high shear sensitivity, zero shear viscosity, melt elasticity, and impact strength.[2] Traditional LCB polymers synthesized by free-radical polymerization processes have very broad molecular weight distributions (MWD), which adversely affect polymer mechanical strengths. The recent advent of metallocene catalysts particularly monocyclopentadienyl type, i.e., Dow Chemical's CGC, has offered a great opportunity for producing LCB polyethylenes with narrow MWD.[3] The active center of the CGC is based on a group IV transition metal (e.g., Ti) covalently bonded to a monocyclopentadienyl ring and bridged with a heteroatom unit, forming a constrained cyclic structure. This geometry allows the transition metal center open to addition of high α-olefins and macromonomers at high reactivities.[4−6] The macromonomers can be formed via chain termination by β-hydride elimination and/or transfer to monomers. The copolymerization of ethylene with the macromonomers produces LCB polymers.

Lai et al.[3] and Swoger et al.[7] reported some initial experimental results utilizing CGC in high-temperature solution CSTR. The advantages of high-temperature homogeneous CSTR processes for LCB include high concentration and low diffusion barrier of macromonomers in the polymerization system.[8] Lai et al.[3] synthesized polyethylene having long chain branching densities (LCBD) in the range 0.01−3 carbons/1000 carbons. These LCB polyethylenes were compared to their Ziegler−Natta counterparts. At narrow polydispersities of 1.5−2.5, the shear thinning I_{10}/I_2 of polyethylene could be increased by introducing more LCB. Swogger et al.[7] synthesized four PE samples with LCB frequencies of 0.20, 0.44, 0.53, and 0.66 per polymer molecule in a CSTR using CGC. Moreover, the synthesis of LCB ethylenes via copolymerization of ethylene with linear and branched high-carbon α-olefins using CGC with MAO as cocatalyst was also reported recently.[9−11]

The LCBD is critical in determining both mechanical and processing properties of polymers. The control of LCBD relies on the understanding of polymerization process and kinetics. In this paper we present the experimental results on the continuous solution polymerization of ethylene using a CGC system.

Experimental Section

CSTR System. Our high pressure, high-temperature CSTR system consists of reactor, control, and data acquisition as shown in Figure 1. An Autoclave Engineers 3 in. inner diameter 600 mL reactor was equipped with a 6-blade 1.25 in. dispersimax and a 1 in. 45° pitched-blade turbine impeller. The maximum working pressure and temperature for this reactor are 3000 psig and 300 °C, respectively. This reactor system has an approximately ideal residence time distribution (RTD). Catalyst, cocatalyst, liquid comonomer, and solvent were fed to the reactor at high pressure by three Neptune 500-S-N3-FA chemical metering pumps and one Neptune 500-D-N3-FA chemical metering pump. The compressor for the gas monomer feed is an Aminco Model 46-14025-1 vertical unit with a maximum operating pressure of 10 000 psig.

Two inlet dip tubes for gas monomer and other reactants, respectively, were installed close to the bottom of the reactor and near the agitator. The outlet dip tube was near the top of the reactor. The *L*/*D* for the reactor is about 1.6. All experiments were carried out at 1000 rpm.

Temperature, pressure, and gas monomer feed rate for the reactor system were controlled by an OPTO 22 Automated Industrial Subsystem. The temperature control was accomplished by an Autoclave Engineers Modular Controller

* To whom correspondence should be addressed at the Department of Chemical Engineering.

10.1021/ma980914u CCC: $15.00
Published on Web 11/19/1998

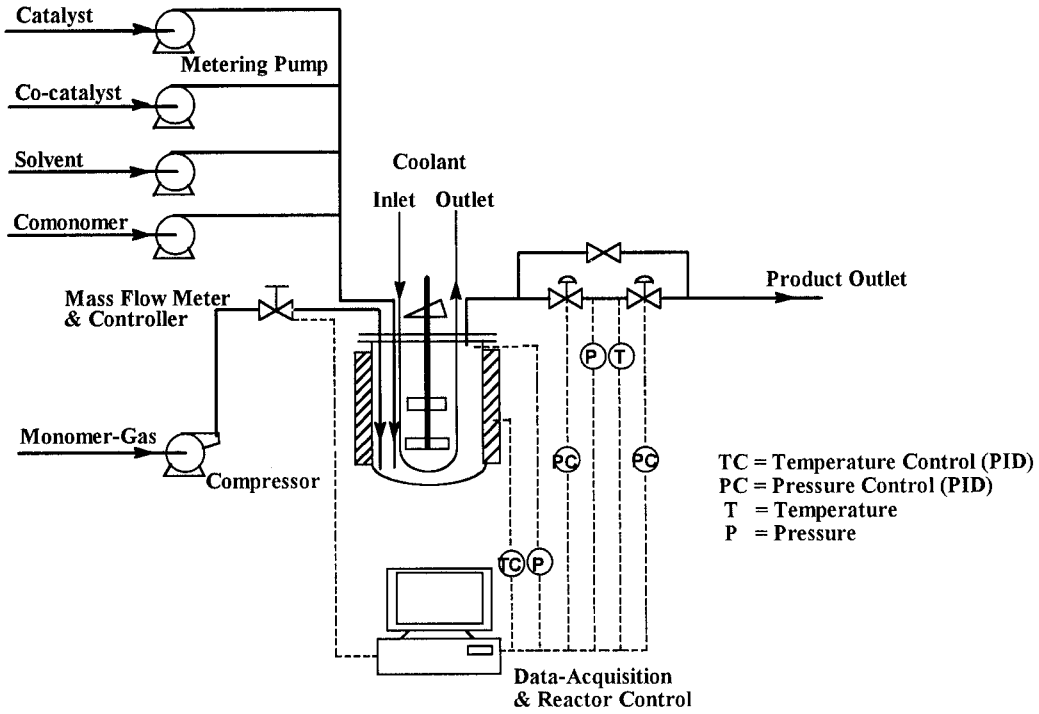

Figure 1. Schematic of the high-pressure high-temperature CSTR system used in this work.

with an integrated circuit control board utilizing a PID algorithm in a time proportional heating of an Autoclave Engineers furnace and the time proportional actuation of a solenoid value for allowing cooling water through the cooling loop in the reactor. The control of pressure was realized using the SCADA (Control and Design) mode of Intellution FIX MMI V 6.0 for Windows 95 software. Fisher Type 646 explosion proof transducers receive a 4−20 mA dc input signal from the OPTO subsystem and transmit a proportional 3−15 psig pneumatic output pressure to the $^1/_4$ in. Badger Type 807 control valve for controlling reactor pressure. The gas monomer feed rate was controlled by a Brooks 5850 TRP mass flow controller. Data acquisition including temperature, pressure, and gas monomer feed rate was realized by the OPTO 22 subsystem. The gas monomer feed rate was acquired by a 1−5 V dc output from the Brooks mass flow controller.

Materials. All manipulations involving air- and moisture-sensitive compounds were carried out under dry nitrogen atmosphere using a glovebox technique. Catalyst, [C_5Me_4-($SiMe_2N^tBu$)]$TiMe_2$ (Me, methyl; ^{t}Bu, *tert*-butyl; C_5, cyclopentadiene) (CGC−Ti), and cocatalyst, tris(pentafluorophenyl)-boron (TPFPB), were provided by Dow Chemical as 10 and 3 wt % solutions in Isopar E, respectively. MMAO-3A was from Akzo-Nobel Corporation as 7.2 wt % aluminum in heptane. The CGC−Ti and cocatalysts were used as received.

Ethylene (polymerization grade > 99.5%) with 560 ppm (in mol) of hydrogen was supplied from Matheson Gas and further purified by passing through columns with CuO from Aldrich to remove oxygen, Ascarite from Fisher Scientific to remove carbon dioxide, and Grace-Davidson molecular sieves to remove moisture. Isopar E (an industrial solvent of hydrocarbons) was supplied from Caledon Laboratories Ltd., dried over a mixture of 5A and 13X molecular sieves from Fisher Scientific and silica gel from Caledon Laboratories Ltd., and de-oxygenated by sparging with ultrahigh purity nitrogen (99.999%) from Matheson Gas.

Polymerization Procedure. All runs were carried out at 500 psig and 140−190 °C. The detail polymerization conditions were summarized in Table 1. The CGC−Ti/MMAO/Isopar E and TPFPB/Isopar E solutions were prepared and stored separately in 1 L catalyst tanks. Solvent, catalyst, and cocatalyst tanks were blanketed with nitrogen and kept at a pressure of 15 mmHg. Three inlet streams, at rates to give the proper average residence time (τ) and desired catalyst and cocatalyst concentrations, were fed into the reactor.

Table 1. Experimental Conditions for the Polymerization Runs in This Work[a]

run no.	T (°C)	τ (min)	ν_E (g/min)	$[M]_0$ (mol/L)	$[H_2]_0$ ($\times 10^4$ mol/L)
1	140	4	6	1.43	8.01
2	140	4	4	0.95	5.34
3	140	4	8	1.90	10.6
4	140	4	10	2.38	13.3
5	140	6	4	1.43	8.01
6	140	8	3	1.43	8.01
7	140	10	2.4	1.43	8.01
8	160	4	6	1.43	8.01
9	180	4	6	1.43	8.01
10	190	4	6	1.43	8.01

[a] Other conditions are pressure (P) = 500 psig, CGC−Ti concentration ([Ti]) = 15 μM, TPFPB concentration ([B]) = 45 μM, and MMAO concentration ([Al]) = 150 μM.

The reactor and system lines were heated to the desired temperature. Isopar E was then fed into the reactor at a gradually increasing rate. After the flow rate of Isopar E reached the 50% of the setting flow and pressure and temperature of the reactor were stabilized, ethylene was charged into the reactor, and the catalyst and cocatalyst pumps were turned on. The time of reaction was set to zero when all the flow rates reached their set points.

During the polymerization process, polymer samples were collected in sampling containers filled with anhydrous ethanol and were then washed with 10-fold amounts of methanol, filtered, and dried under vacuum.

Characterization. ^{13}C NMR spectra were obtained at 120 °C, using a Bruker AC 300 pulsed NMR spectrometer with broad band decoupling at 75.4 MHz. The sample concentrations were over 35 wt % in deuterated *o*-dichlorobenzene (ODCB-*d*) and 1,2,4-trichlorobenzene (TCB) using 10-mm sample tubes. Chemical shifts were referenced internally to TCB and lock was provided by ODCB-*d*. Spectra required more than 7000 scans to attain an acceptable signal-to-noise ratio. As the spin−lattice relaxation time (T_1) of the major carbons in polyethylene are less than 2 s at present conditions, a delay time between pulses of 10 s was used. Due to the saturation effect, the integral areas of terminal methyl (1s) and methylene (2s) groups should be multiplied by the correction factor, where T_1 = 6.05 s for 1s and 4.52 s for 2s.

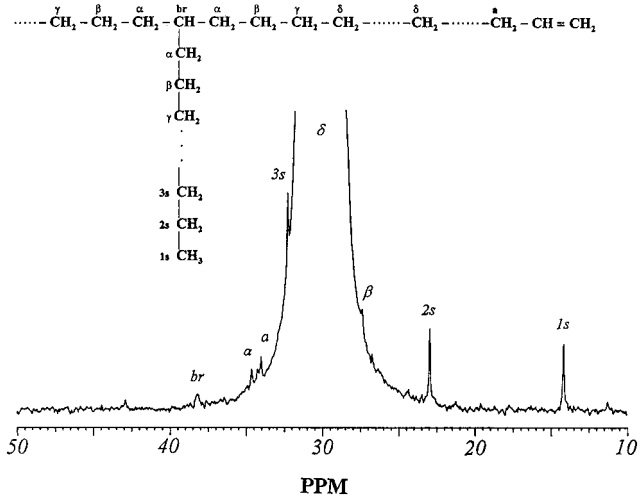

Figure 2. ^{13}C NMR spectrum of PE sample (run 6) measured at 120 °C using deuterium *o*-dichlorobenzene and 1,2,4-trichlorobenzene as solvents.

Figure 2 gives the spectrum of a LCB PE sample prepared at 140 °C (run 6) and the assignment of different chemical shifts.[12−15] In the integration of the resonance peaks close to the peak $\delta\delta^+$, the baseline effect by the "tree trunk" of peak $\delta\delta^+$ was subtracted from the signals. The long chain branching density (LCBD, the number of branching points per carbon), saturated chain end density (SCED, the number of saturated chain ends per carbon), unsaturated chain end density (UCED, the number of unsaturated chain ends per carbon), long chain branching frequency (LCBF, the number of branching points per polymer molecule) and concentration of macromonomers ($[P^{2-}]$) were calculated using the equations

$$\mathrm{LCBD} = \frac{\mathrm{IA}_a}{3\mathrm{IA}_{\mathrm{Tot}}} \tag{1}$$

$$\mathrm{SCED} = \frac{(\mathrm{IA}_{1s} + \mathrm{IA}_{2s})}{2\mathrm{IA}_{\mathrm{Tot}}} \tag{2}$$

$$\mathrm{UCED} = \frac{\mathrm{IA}_a}{\mathrm{IA}_{\mathrm{Tot}}} \tag{3}$$

$$\mathrm{LCBF} = \frac{2\mathrm{LCBD}}{\mathrm{SCED} + \mathrm{UCED} - \mathrm{LCBD}} \tag{4}$$

$$[P^{2-}] = 2([M]_0 - [M])\mathrm{UCED} \tag{5}$$

where IA_α, IA_{1s}, IA_{2s}, IA_a and IA_{Tot} are the integral areas of α, 1s, 2s, a-CH_2 resonances, and total intensity of carbons, respectively, $[M]_0$ and [M] are the inlet and outlet ethylene concentrations. [M] was calculated from $[M]_0$ and conversion (x) by $[M] = [M]_0(1 - x)$.

Molecular weight (MW) and MWD of the polymers were measured by a Waters-Millipore 150 C High-Temperature SEC in TCB at 140 °C and a flow rate of 1 mL/min, using differential refractive index detector. The SEC was equipped with three linear mixed Shodex AT806MS columns. The concentrations of polymer samples were 0.1 wt %. Calibration was performed at 140 °C against the known monodisperse TSK polystyrene (PS) standards from TOYO SODA Mfg. Co. with MW of 775, 422, 42.8, 6.2, and 2.8 kg/mol. The Mark−Houwink constants for the universal calibration curve were $K = 2.32 \times 10^{-4}$ and $\alpha = 0.653$ for PS and $K = 3.95 \times 10^{-4}$ and $\alpha = 0.726$ for PE.

Melt flow indexes, I_2 and I_{10}, were measured at 190 °C in a Kayeness Inc. Model D-0053 Melt Indexer according to the ASTM D 1238-90b.[16] The testing loads for I_2 and I_{10} were 2.16 and 10 kg, respectively. All PE samples were mixed with 0.6 wt % Irganox 1010.

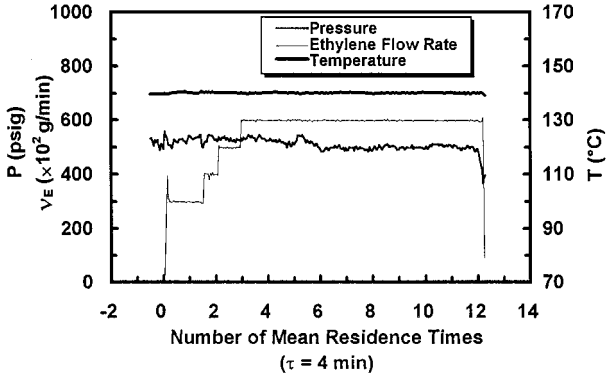

Figure 3. Date acquisition from run 1 showing reactor temperature (T), pressure (P), and ethylene feed rate (ν_E) during polymerization process. The experimental conditions: $P = 500$ psig, $T = 140$ °C, $\nu_E = 6$ g/min, $\tau = 4$ min, [Ti] = 15 μM, [B] = 45 μM, and [Al] = 150 μM.

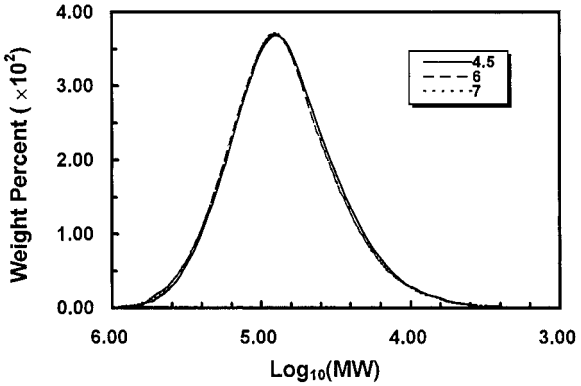

Figure 4. High-temperature GPC curves of PEs taken from run 1. Three PE samples were collected at 4.5, 6, and 7 times τ after the start of polymerization. The conditions are the same as Figure 3.

Results and Discussion

Process Control and Stability. Figure 3 shows a typical example for the change of temperature (T), pressure (P) and ethylene feed rate (ν_E) during polymerization using our CSTR system (run 1). All the three variables were in good control and reached steady state after four mean residence times of the reactor. Figure 4 shows the GPC curves of PE samples collected at three different τ's for run 1. Figure 5 shows the corresponding melt flow index (I_2), index ratio (I_{10}/I_2) and ethylene conversion. It can be noted that the GPC curves and ethylene conversion remained unchanged and the values of I_2 and I_{10}/I_2 were also reasonably close after 4 τ's. This indicates the reactor system reached a steady state at 4 τ's of polymerization time and the catalyst kept the same active-site type during the polymerization. The stability of operation for the current CGC was similar to that for Cp_2ZrCl_2/MMAO/TMA using the same CSTR system reported earlier.[1] All the polymer samples for the measurements of melt flow index, GPC and ^{13}C NMR reported in this paper were collected between 7 and 8 τ's.

Catalyst Activity and Molecular Weight. The polymerization rate, activity, GPC measurement and melt flow index data for the total 10 runs are summarized in Table 2. The activities were from 3.19 to 11.5 kg of PE/(g of CGC−Ti) or from 1200 to 15600 kg

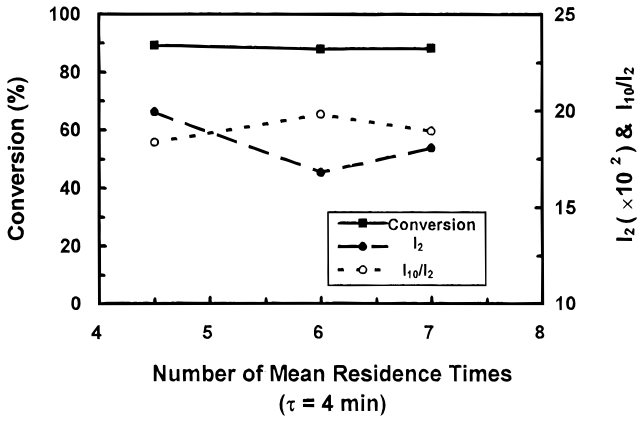

Figure 5. Effect of the number of mean residence times (τ's) on ethylene conversion, melt flow index (I_2) and ratio (I_{10}/I_2) for run 1. The conditions are the same as Figure 4.

of PE/([M]·mol of Ti) (from 3.66 to 47.6 kg of PE/([M]·g of catalyst)). In comparison, the average activity of 187 kg of PE/([M]·g of catalyst) for zirconocene, Cp_2ZrCl_2/MMAO/TMA, was reported using the same CSTR system.[1] The activity of CGC−Ti appeared to be lower than that of Cp_2ZrCl_2.

The GPC measurements gave the weight-average molecular weights (M_w) in the range $(0.94-1.29) \times 10^5$ g/mol. The polydispersities were close to 2, approximating Flory's most probable distribution and suggesting a single site type for the CGC−Ti catalyst system. It is known that the GPC technique using a differential refractive index detector does not give accurate molecular weights for branched polymers. A branched polymer assumes smaller coil in a good solvent than its linear counterpart with the same molecular weight. The technique thus underestimates the molecular weight for the branched polymers. The GPC data listed in Table 2 should be considered as approximate values for the polymer samples.

The melt flow index data I_2 are also indicative of the polymer molecular weights: the higher the molecular weight, the lower the I_2 is for polymer samples having the same branching density. The polyethylenes made in this work gave very low I_2 values; most of them were in the range of 0.1−0.3 g per 10 min due to their high molecular weights and, more importantly, the effect of long chain branching. An examination of the M_w and I_2 data in Table 2 reveals that the lower I_2 values of runs 1−7 than runs 8−10 are mainly contributed by higher LCBDs of runs 1−7 because all the runs 1−10 produced polyethylenes with the same M_w level. The ratio of I_{10} and I_2 is a rheological measurement of LCB. A narrowly distributed linear polyethylene normally gives a I_{10}/I_2 value in the range of 6−8. Our samples have I_{10}/I_2 values up to 25.7 (run 6), indicating the presence of LCB. Table 3 gives the LCBD and LCBF data for the polymer samples made in this work. The correlation of the I_{10}/I_2 and LCBD is evident. It is rather surprising to see such a strong effect of LCB on the polymer rheological properties considering most of the samples having very low branching densities, one branch per 5−10 polymer molecules. The detailed analysis of the rheological and mechanical properties of the branched polyethylenes has been published elsewhere.[17]

The effects of ethylene feed concentration ($[M]_0$) on the catalyst activity and polymer molecular weight are demonstrated in Table 2 (runs 1−4). Four levels of the feed rate were investigated: 4 (run 2), 6 (run 1), 8 (run 3), and 10 g/min (run 4). The effect of $[M]_0$ on the I_2 and I_{10}/I_2 appeared to be significant, indicating the levels of branching increased with $[M]_0$.

The effects of the mean residence time (τ) are shown in runs 1 and 5−7. Four levels of the mean residence time were used: 4 (run 1), 6 (run 5), 8 (run 6), and 10 min (run 7). The ethylene conversion decreased significantly with increasing τ exhibited the catalyst deactivation. The changes of I_2 and I_{10}/I_2 with τ appeared to be more complicated, with run 6 giving the lowest I_2 and highest I_{10}/I_2, consistent with the highest LCBD in Table 3.

The temperature effects were also studied at 140 (run 1), 160 (run 8), 180 (run 9), and 190 °C (run 10): The low ethylene conversions in runs 8−10 indicate that the deactivation of the CGC−Ti catalyst system is severe at high temperatures. The polymers produced at the elevated temperatures were more linear having very low LCBDs and I_{10}/I_2 values. The lack of LCB formation is due to the low macromonomer concentration relative to ethylene.

Polymerization Scheme and Kinetic Analysis. The following elementary reactions are possibly involved in the present polymerization process

$$\text{activation/reactivation:}\quad A + M \xrightarrow{k_a} P^* \qquad R_a = k_a[A][M] \quad (6)$$

$$\text{propagation:}\quad P^* + M \xrightarrow{k_p} P^* \qquad R_p = k_p[P^*][M] \quad (7)$$

β-hydride elimination:

$$P^* \xrightarrow{k_\beta} P^{2-} + A \qquad R_\beta = k_\beta[P^*] \quad (8)$$

$$\text{transfer to monomer:}\quad P^* + M \xrightarrow{k_{fM}} P^{2-} + P^* \qquad R_{fM} = k_{fM}[P^*][M] \quad (9)$$

$$\text{long chain branching:}\quad P^* + P^{2-} \xrightarrow{k_{LCB}} P^* \qquad R_{LCB} = k_{LCB}[P^*][P^{2-}] \quad (10)$$

$$\text{transfer to hydrogen:}\quad P^* + H_2 \xrightarrow{k_{fH}} P + A \qquad R_{fH} = k_{fH}[P^*][H_2] \quad (11)$$

$$\text{transfer to MAO:}\quad P^* + Al{-}R \xrightarrow{k_{fAl}} P + P^* \qquad R_{fAl} = k_{fAl}[P^*][Al] \quad (12)$$

$$\text{deactivation: active site} \xrightarrow{k_{dA}} \text{inert} \quad (13)$$

where R_i and k_i (i = a, p, β, fM, LCB, fH, fAl and dA) are the reaction rates and rate constants, respectively, and [A], [P*], [H_2], [Al], and [P] denote the concentrations of active site, propagating center, hydrogen, aluminoxane, and dead polymer chain, respectively. For the long chain branching formation, we believe that the ethylene macromonomers, once generated, are "in situ" incorporated into growing polymer chains to form branches before they diffuse out of the vicinity of the active center. This is why LCB metallocene polyethylenes can also be made by gas-phase and slurry processes.

Our experimental data in Table 2 showed that the ethylene conversion decreased with increasing the mean

Table 2. Summary of Conversion, Activity, and GPC and Melt Flow Index Data

run no.	x (%)	[M] (mol/L)	R_p ($\times 10^3$ mol/L sec)	activity (kg of PE/ g of CGC−Ti)	activity ($\times 10^{-3}$ kg of PE/ [M]·mol of Ti)	M_w ($\times 10^{-5}$)	M_w/M_n	I_2 (g/10 min)	I_{10}/I_2
1	89.3	0.153	5.31	7.27	15.6	1.04	2.04	0.206	17.8
2	80.7	0.184	3.20	4.38	7.82	1.02	2.01	0.276	17.7
3	86.1	0.265	6.83	9.35	11.5	1.15	2.04	0.136	20.9
4	84.7	0.364	8.40	11.5	10.3	1.09	2.00	0.107	22.3
5	80.9	0.273	3.21	6.59	7.91	1.13	1.99	0.158	18.6
6	80.8	0.275	2.41	6.58	7.85	1.13	2.09	0.081	25.7
7	66.7	0.476	1.59	5.43	3.73	1.29	2.02	0.192	13.3
8	74.5	0.365	4.43	6.07	5.45	1.02	1.98	0.626	11.8
9	44.8	0.789	2.67	3.65	1.51	1.05	1.84	1.12	7.64
10	39.2	0.869	2.33	3.19	1.20	0.94	1.88	2.02	7.41

residence time. This result indicates that the deactivation of catalyst does not follow a simple first-order kinetics. In this work, the following empirical deactivation function is assumed:

$$[P^*] = [A]_0 \exp(-k_d\tau) \tag{14}$$

The assumption of $[P^*] \gg [A]$, implied in eq 14, is believed to be reasonable under the experimental conditions of this work where the polymerization system was not monomer starving. Substituting eq 14 into eq 7 (similarly $[M]_0 - [M] = k_p [P^*][M]\tau$) results in

$$\ln\{\tau[A]_0(1 - x)/x\} = k_d\tau - \ln k_p \tag{15}$$

Equation 15 gives the estimate of k_p and k_d.

The amount of LCBD in PE depends on the competition between monomer and macromonomer propagation, which are shown in eqs 7 and 10, respectively. The ratio of two propagation rate coefficients can be, therefore, calculated using the LCBD value.

$$\frac{k_{LCB}[P^{2-}]}{2k_p[M]} = \text{LCBD} \tag{16}$$

The ratio of the generation of macromonomer over that of monomer propagation can also be estimated from the NMR data:

$$\frac{k_\beta + k_{fM}[M]}{2k_p[M]} = \text{UCED} + \text{LCBD} \tag{17}$$

$$\frac{k_{fH}[H_2] + k_{fAl}[Al]}{2k_p[M]} = \frac{\text{SCED} - (\text{LCBF} + 1)\text{UCED}}{\text{LCBF} + 2} \tag{18}$$

On the basis of the mass balances for H_2, $[H_2]_0 - [H_2] = k_{fH}[P^*][H_2]\tau$, and for ethylene monomer, $[H_2]$ can be calculated using the following equation:

$$[H_2] = \frac{[H_2]_0}{\frac{k_{fH}}{k_p}\frac{x}{(1 - x)} + 1} \tag{19}$$

Estimate of Reaction Rate Constants. Figure 6 shows the plot of $\ln\{\tau[A]_0(1 - x)/x\}$ vs τ. The slope and intercept as well as their 90% confidence ranges of the curve give $k_p = 5.73 \times 10^3$ [(3.38−9.69) $\times 10^3$] L mol^{-1} s^{-1} and $k_d = (5.22 \pm 1.43) \times 10^{-3}$ s^{-1} for the CGC−Ti catalyst at 140 °C. Compared to the zirconocene system in our previous work ($k_d = 2.1 \times 10^{-3}$ s^{-1}),[1] the CGC−Ti catalyst exhibited more severe deactivation. However, comparisons of k_p values are not straightforward

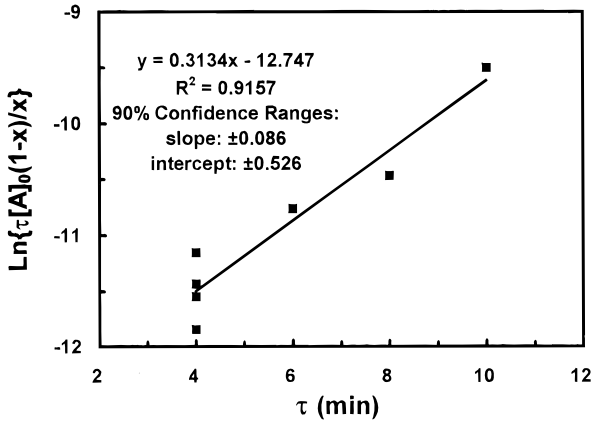

Figure 6. Plot of $\ln\{\tau[A]_0(1 - x)/x\}$ vs τ to estimate the rate constants for ethylene propagation and catalyst deactivation at 140 °C. The points are experimental data and the curve is the linear least-squares regression fit.

Table 3. Summary of ^{13}C NMR Data

run no.	LCBD ($\times 10^4$)	SCBD ($\times 10^4$)	SCED ($\times 10^4$)	UCED ($\times 10^4$)	LCBF	[P^{2-}] ($\times 10^4$ mol/L)
1	0.35	0	6.06	0.65	0.11	1.66
3	0.38	0	5.66	0.79	0.12	2.58
4	0.40	0	5.45	0.84	0.14	3.39
1	0.35	0	6.06	0.65	0.11	1.66
6	0.44	0	4.65	1.35	0.16	3.12
7	0.20	0	5.06	1.02	0.07	1.95
1	0.35	0	6.06	0.65	0.11	1.66
8	0.22	0	5.43	1.09	0.07	2.32
9	0.20	0.53	5.36	1.73	0.06	2.22
10	0.21	0.79	5.29	2.20	0.06	2.47

Table 4. Estimated Ratio of LCB and Ethylene Propagation Rate Constants

run no.	T (°C)	LCBD ($\times 10^4$)	[M] (mol/L)	[P^{2-}] ($\times 10^4$ mol/L)	k_{LCB}/k_p ($\times 10^2$)
1	140	0.35	0.153	1.66	6.45
3	140	0.38	0.265	2.58	7.81
4	140	0.40	0.364	3.39	8.59
6	140	0.44	0.275	3.12	7.82
7	140	0.20	0.476	1.95	9.78
8	160	0.22	0.365	2.32	6.92
9	180	0.20	0.789	2.22	14.2
10	190	0.21	0.869	2.47	14.8

since they were estimated in different manners. The estimated k_p for the zirconocene system included the effect of catalyst deactivation.

The ratios of LCB and ethylene propagation rate constants, k_{LCB}/k_p, are estimated using eq 16 and the data of [M] in Table 2 and [P^{2-}] and LCBD in Table 3. Table 4 lists these rate constant values under various experimental conditions. At 140 °C, the k_{LCB}/k_p values are in the range 0.0624−0.0978. The average value is therefore 0.0809 ± 0.0185, indicating the open structure

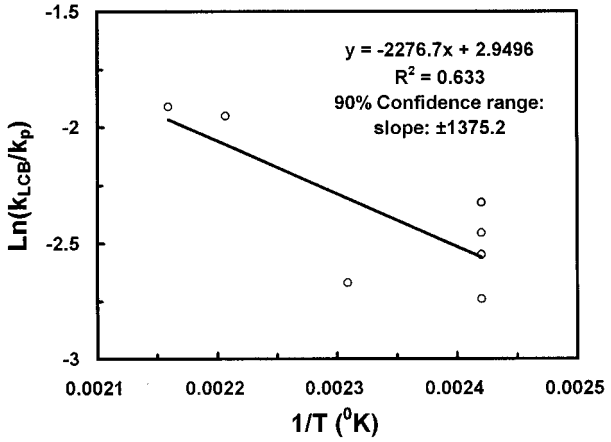

Figure 7. Arrhenius relationships for k_{LBC}/k_p.

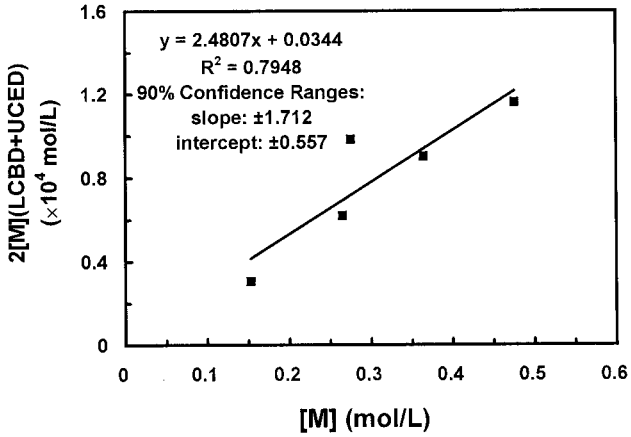

Figure 8. Plot of 2[M](LCBD + UCED) vs [M] to estimate the rate constant of PE chain termination by transfer to monomer and β-hydride elimination at 140 °C. The points are experimental data and the curve is the linear least-squares regression fit.

of CGC−Ti catalyst permits significant incorporation of high molecular weight macromonomers. The effect of temperature on k_{LCB}/k_p is evident in Table 4. Assuming an Arrhenius type of temperature dependence for both LCB formation and ethylene propagation

$$k_{LCB}/k_p = (A_{LCB}/A_p) \exp(-\Delta E/RT) \qquad (20)$$

we plot $\ln(k_{LCB}/k_p)$ vs $1/T$ in Figure 7. The slope gives an activation energy difference between LCB and ethylene propagation of $\Delta E/R = (2.28 \pm 1.38) \times 10^3$ K.

The use of eq 17 and NMR data (UCED and LCBD) in Table 3 allows one to estimate the ratio of β-hydride elimination and transfer to monomer over ethylene propagation rate constants, k_β/k_p and k_{fM}/k_p. Figure 8 plots 2[M](UCED + LCBD) vs [M]. The slope and intercept of the curve give the estimates $k_{fM}/k_p = (2.48 \pm 1.71) \times 10^{-4}$ and $k_\beta/k_p = (0.344 \pm 5.57) \times 10^{-5}$ L/mol, respectively, for the CGC−Ti catalyst system at 140 °C. The results demonstrate that most terminal vinyl groups were formed by transfer to monomer and β-hydride elimination was minor under the experimental conditions of the present study. Compared to $k_{fM}/k_p = 9.4 \times 10^{-4}$ and $k_\beta/k_p = 5.8 \times 10^{-4}$ L/mol for the Cp_2ZrCl_2 catalyst,[1] these values are rather small, indicating the preferable use of zirconocene for macromonomer generation. These observations resort to the use of binary metallocene systems in synthesizing LCB polyethylenes with one catalyst (e.g. conventional zirconocene) generating polymer chains by β-hydride elimination and the other (e.g. CGC−Ti) in situ propagating with the terminal double bonds. Our theoretical work[18] showed that the branched polymers thus produced give much narrower molecular weight distributions than random polymers with the same branching densities synthesized by a single catalyst system. The distribution shows a rather sharp truncation at the high molecular weight end, while the latter has a long skew tail which may cause difficulty in processing. The experimental work of a binary metallocene catalyst system has been carried out recently and will be published elsewhere.[19]

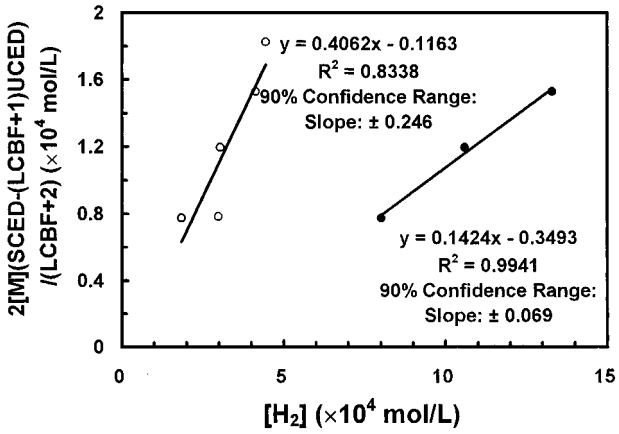

Figure 9. Plot of 2[M](SCED − (LCBF + 1)UCED)/(LCBF + 2) vs $[H_2]$ to estimate the rate constant of PE chain termination by transfer to hydrogen. The points are experimental data (solid symbols for $[H_2]_0$ and empty ones for $[H_2]$), and the curve is the linear least-squares regression fit.

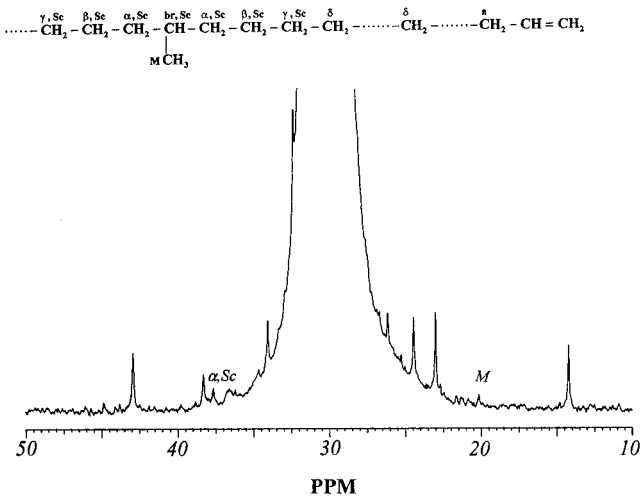

Figure 10. ^{13}C NMR spectrum of PE sample (run 10) measured at 120 °C using deuterium *o*-dichlorobenzene and 1,2,4-trichlorobenzene as solvents. It shows the presence of methyl side chains.

The estimate of the transfer to hydrogen rate constant k_{fH}/k_p from Table 3 requires some iteration steps using eqs 18 and 19. We first plot 2[M](SCED − (LCBF + 1)UCED)/(LCBF + 2) vs $[H_2]_0$ at the same τ and different $[M]_0$ according to eq 18 and then use the slope of the curve to adjust hydrogen concentrations by eq 19. Repeating this procedure eventually results in a converged value of $k_{fH}/k_p = 0.406 \pm 0.246$. Polymer chains terminated by other mechanisms such as transfer to aluminoxane and deactivation appear to be negligible.

Short Chain Branching at High Temperatures. It is rather interesting to note that methyl side chains

were present in the PE samples synthesized at high temperatures. Figure 10 shows a ^{13}C NMR spectrum of PE sample produced at 190 °C and the assignment of chemical shifts.[12,13] The resonances at 37.6 and 20.1 ppm, due to α-CH_2 adjacent to methine group of methyl side chain and the CH_3 of methyl group, can be clearly seen in the spectrum. The short chain branching density (SCBD, the number of branching points per carbon) can be estimated using

$$\mathrm{SCBD} = \frac{\mathrm{IA}_{\alpha,\mathrm{sc}}}{2\mathrm{IA}_{\mathrm{Tot}}} \tag{21}$$

The SCBD values listed in Table 3 for runs 9 and 10 were 0.53 and 0.79 per 10 000 carbons, higher than their respective LCBD levels. No significant short chain branching was observed at temperatures below 180 °C.

To explain the formation of methyl side chains, we speculate in situ 2,1-insertion of macromolecule following β-hydride elimination:

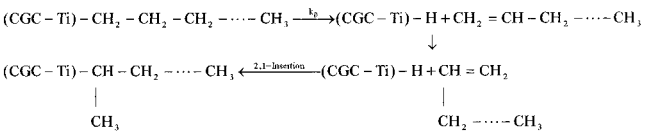

This mechanism is possible only at an active site with very open structure and little steric hindrance like the CGC−Ti catalyst system in this work and high temperatures which provide adequate energies for macromonomer to rotate. Similar mechanisms for methyl side chain formation have been discussed in ethylene polymerization using nitrogen-ligated Ni(II)- and Pd(II)-based catalysts.[20−23]

Conclusions

Using our high temperature high pressure CSTR system with an approximately ideal RTD and Dow Chemical's constrained geometry catalyst, CGC−Ti/TPFPB/MMAO, we produced polyethylenes with LCBDs up to 0.44 carbons/10 000 carbons, shear thinning of $I_{10}/I_2 = 7.4-25.7$, and a narrow PDI of about 2. All the polymerization runs showed good control over the reaction variables, and reached the steady state after 4 mean residence times. The CGC−Ti catalyst appeared to be single site type. The major mechanism for macromonomer formation was found to be transfer to monomer with β-hydride elimination played a minor role. The open structure of the catalyst system permitted ethylene macromonomers to be incorporated to form LCB. Short chain branching with methyl side chains was also observed at high temperatures, and believed to be introduced by 2,1-insertion following β-hydride elimination.

Under the experimental conditions at 140 °C, the CGC−Ti catalyst system appeared to be rather active with $k_p = 5.73 \times 10^3$ [$(3.38-9.69) \times 10^3$] L mol^{-1} s^{-1}. Significant deactivation of the catalyst was also observed obeying an exponential decay with $k_d = (5.22 \pm 1.43) \times 10^{-3}$ s^{-1}. The ratio of the rate constants of LCB and monomer propagation was estimated $k_{LCB}/k_p = (8.09 \pm 1.85) \times 10^{-2}$ with an activation energy $\Delta E/R = (2.28 \pm 1.38) \times 10^3$ K. The rate constants of β-hydride elimination, transfer to monomer, and transfer to hydrogen were also estimated: $k_\beta/k_p = (0.344 \pm 5.57) \times 10^{-5}$ L/mol, $k_{fM}/k_p = (2.48 \pm 1.71) \times 10^{-4}$, and $k_{fH}/k_p = 0.406 \pm 0.246$, respectively.

Acknowledgment. The authors are grateful to the National Science and Engineering Research Council of Canada (NSERC) for support for this research. Thanks are given to Prof. Brian G. Sayer for help in the NMR measurements.

References and Notes

(1) Charpentier, P. A.; Zhu, S.; Hamielec, A. E.; Brook, M. *Ind. Eng. Chem. Res.* **1997**, *36*, 5074.
(2) Small, P. A. *Adv. Polym. Sci.* **1975**, 18, 1.
(3) Lai, S. Y.; Wilson, J. R.; Knight, G. W.; Stevens, J. C.; Chum, P. W. S. (to Dow Chemical Co.). Elastic substantially linear olefin polymers. U.S. Patent 5,272,236, 1993.
(4) Knight, G. W.; Lai, S. Polyolefins VIII. *Technol. Pap., Reg. Technol. Conf.—Soc. Plast. Eng.* **1993**, 28.
(5) Shiono, T.; Moriki, Y.; Soga, K. *Macromol. Symp.* **1995**, *97*, 161.
(6) Woo, T. K.; Fan, L.; Ziegler, T. *Organometallics* **1994**, *13*, 2252.
(7) Swogger, K.; Kao, W. C. I. Polyolefins VIII. *Technol. Pap., Reg. Technol. Conf.—Soc. Plast. Eng.* **1993**, 14.
(8) Soares, J. P.; Hamielec, A. E. *Macromol. Theory Simul.* **1996**, *5*, 547.
(9) Brant, P.; Canich, J. A. M. Ethylene/Longer α-Olefin Copolymers. U.S. Patent 5,475,075, 1995.
(10) Brant, P.; Canich, J. A. M.; Merrill, N. A. (to Exxon Chemical Patents Inc.). Ethylene/Branched Olefin Copolymers. U.S. Patent 5,444,145, 1995.
(11) Sugawara, M. In *Proceedings of the 4th International Business Forum on Specialty Polyolefins*; Houston, TX, 1994; p 37.
(12) ASTM D 5017-91. Determination of Linear Low-Density Polyethylene (LLDPE) Composition by Carbon-13 Nuclear Magnetic Resonance. 1991.
(13) De Pooter, M.; Smith, P. B.; Dohrer, K. K.; Bennett, K. F.; Meadows, M. D.; Smith, C. G.; Schouwenaars, H. P.; Geerards, R. A. *J. Appl. Polym. Sci.* **1991**, *42*, 399,
(14) Hansen, E. W.; Blom, R.; Bade, O. M. *Polymer* **1997**, *38*, 4295.
(15) Randall, J. C.; Zoepfl, F. J.; Silverman, J. A ^{13}C NMR Study of Radiation-Induced Structural Changes in Polyethylene. In *ACS Symposium* Series 249; Randall, J. C., Ed.; American Chemical Society: Washington, DC, 1984; Chapter 16.
(16) ASTM D 1238-90b. Flow Rates of Thermoplastics by Extrusion Plastometer. 1990.
(17) Yan, D.; Wang, W.-J.; Zhu, S.; Hamielec, A. E. Rheological and Mechanical Properties of Long-Chain Branched Polyethylene Produced by High-Temperature Solution Polymerization Using Dow's Constrained Geometry Catalysts. *Polymer*, in press.
(18) Zhu, S.; Li, D. *Macromol. Theory Simul.* **1997**, *6*, 793.
(19) Wang, W.-J.; Yan, D.; Zhu, S.; Hamielec, A. E. Long Chain Branching in Ethylene Polymerization Using Binary Metallocene Catalyst System. Submitted for publication in *Polym. React. Eng.* **1998**.
(20) De Souza, R. F.; Mauler, R. S.; Simon, L. C.; Nunes, F. F.; Vescia, D. V. S.; Cavagnolli, A. *Macromol. Rapid Commun.* **1997**, *18*, 795.
(21) Deng, L.; Margl, P.; Ziegler, T. *J. Am. Chem. Soc.* **1997**, *119*, 1094.
(22) Johnson, L. K.; Killian, C. M.; Brookhart, M. *J. Am. Chem. Soc.* **1995**, *117*, 6414.
(23) Musaev, D. G.; Froese, R. D. J.; Svensson, M.; Morokuma, K. *J. Am. Chem. Soc.* **1997**, *119*, 367.

MA980914U